November 1, 1991

Detection of unresolved target tracks in infrared imagery

Sarah A. Rajala, *North Carolina State University*
Loren W. Nolte, *Duke University*
James V. Aanstoos

Detection of unresolved target tracks in infrared imagery

Sarah A. Rajala

North Carolina State University, Dept. of Electrical and Computer Engineering
Box 7911, Raleigh, NC 27695-7911

Loren W. Nolte

Duke University, Dept. of Electrical Engineering Durham, NC 27706

James V. Aanstoos

Research Triangle Institute, P.O. Box 12194, Research Triangle Park, NC 27709

ABSTRACT

Two methods for detecting dim, unresolved target tracks in infrared imagery are presented. Detecting such targets in a sequence of noisy images is very challenging from the standpoint of algorithm design as well as detection performance evaluation. Since the signal-to-noise ratio per pixel is very low (a dim target) and the target is unresolved (of spatial extent less than a pixel), one must rely on integration over target tracks which span over many image frames. In addition, since there is a large amount of uncertainty as to the pattern and location of target tracks, good algorithms must consider a large number of possibilities. The first method is based on a generalization of the Hough transform-based algorithm using the Radon transform. The second approach is an extension of a detection theory algorithm to 3-D. Both algorithms use a 3-D volume of spatial-temporal data.

1. INTRODUCTION

The problem addressed in this paper is the detection of dim, unresolved target tracks in infrared imagery. In such problems, two-dimensional digital image frames of the same field of view are collected at short, periodic intervals. A target (if present) usually moves in a direction approximately perpendicular to the sensor line of sight (so its size is constant) and moves through the field of view while the background stays relatively constant. If a target is in the field of view, it appears in a succession of frames as it moves. In each frame in which a target appears, it shows up in one or a few pixels, depending on its size, its speed, and the point spread function of the optics. The result is a three-dimensional set of data containing noise and, if there is a target, a signal of constant or time-varying amplitude. Detecting such targets in a sequence of noisy images is challenging from the standpoint of algorithm development as well as detection performance evaluation. Since the signal-to-noise ratio (SNR) per pixel is very low (a dim target) and the target is unresolved (of spatial extent less than a pixel), one must rely on integration over target tracks which span many image frames. In addition, since there is a large amount of uncertainty as to the pattern and location of target tracks, good algorithms must consider a large number of possibilities.

During the last several years, the authors have participated in a joint effort to propose solutions to the problem of detecting dim, unresolved target tracks. In the first phase, a Hough transform-based algorithm for extracting the target tracks was developed and the results presented in [1]. The performance of the algorithm was evaluated using data containing varying amounts of system noise, background clutter, and spacecraft jitter. The results show that this algorithm performs well under a variety of conditions, but as the SNR is reduced significantly the performance degrades rapidly. Later, the Hough transform-based algorithm was generalized to detect linear and curved tracks [2]. In parallel with this effort, the track detection problem was reformulated as a two-hypothesis detection theory problem. This reformulation provides alternative methods for evaluating algorithm performance (e.g., probability of detection, probability of false alarm, and a posteriori probabilities), an optimal algorithm for detecting and localizing tracks, and incorporates, as a subset, the Hough transform algorithm [3], [4], [5]. Each of these algorithms has been evaluated using sets of 2-D track map sequences. A track map sequence results from projecting a preprocessed time sequence of image frames onto one 2-D track map image. The track map data may still contain some noise;

 0-8194-0743-7/91/$4.00

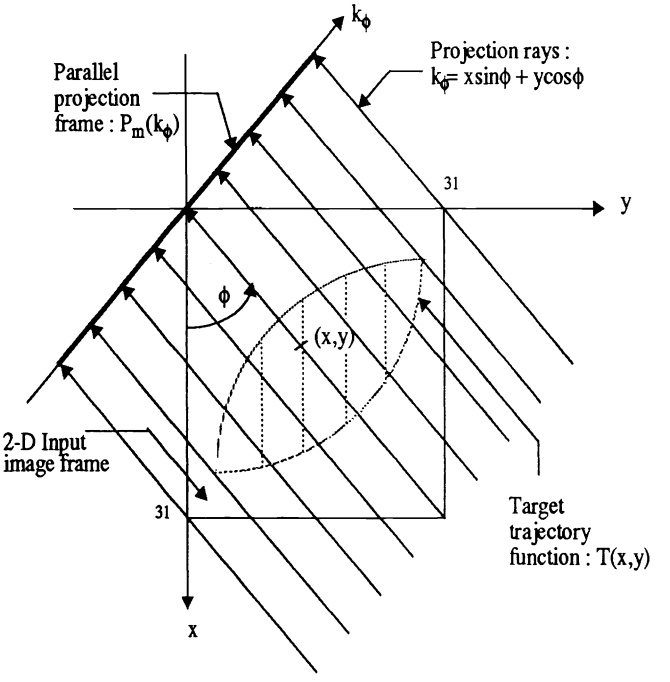

Figure 1: Two-dimensional geometry of Radon-like forward parallel projection.

however, it is assumed that the remaining noise is white. The results show good performance for both the Hough transform-based and the detection theory algorithms, with better performance from the detection theory algorithm especially at low signal-to-noise ratios (SNRs).

There is a limitation, however, in overall performance when using temporal projection to create a 2-D track map sequence from the original 3-D (space and time) image data, especially when the targets are dim. Even if the projection is performed optimally, it causes a significant reduction in the effective SNR as compared to the SNR of the original 3-D data. In this paper, two approaches for circumventing this problem will be presented. The first approach is based on an extension of the Hough transform-based algorithm using the Radon transform. The second approach is an extension of the detection theory algorithm to 3-D.

2. PROJECTION-BASED HOUGH TRANSFORM

In this section a projection-based Hough transform algorithm derived from the Radon transform is presented. Here, the Radon transform provides a mechanism for obtaining a set of projections at arbitrary angles. Computing the Radon transform consists of computing the projections of an image along a particular pattern, e.g., a straight line. Mathematically the problem can be stated as follows. Let T(x,y) represent a two-dimensional function. As shown in Figure 1, a line running through T(x,y) is called a *ray*. The integral of T(x,y) along a ray is called a *ray integral*, and a set of ray integrals forms a *projection*.

The equation for an individual ray is given by

$$k_\phi = x sin\phi + y cos\phi \tag{1}$$

where k_ϕ is the perpendicular distance of the ray from the origin. The integral of the function T(x,y) along this ray

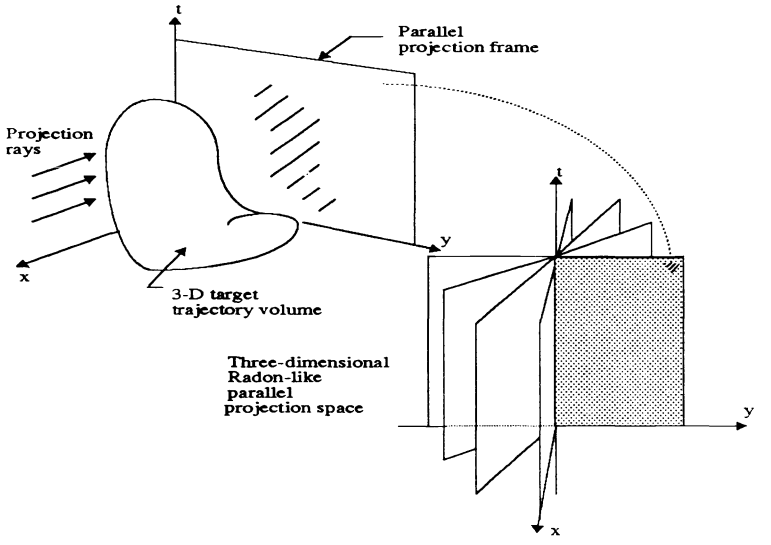

Figure 2: Radon-like forward parallel projection.

may be expressed as

$$P(k_\phi) = \int_{\mathbf{ray}} T(x,y)d^2\mathbf{r} = \int_{\infty}^{\infty}\int_{\infty}^{\infty} T(x,y)\delta(xsin\phi + ycos\phi - k_\phi)dxdy. \tag{2}$$

The function $P(k_\phi)$ as a function of k_ϕ (for a given value of ϕ) is the parallel projection of T(x,y) for angle ϕ. The one-dimensional function $P(k_\phi)$ is also called the *Radon transform* of T(x,y). A projection taken along a set of parallel rays is called a *parallel projection*, an example of which is shown in Figure 2.

Eq. 2 is generalized to a three-dimensional Radon transform as shown below

$$P(k_\phi,t) = \int_{\mathbf{plane}} T(x,y,t)d^3\mathbf{r} = \int_{\infty}^{\infty}\int_{\infty}^{\infty}\int_{\infty}^{\infty} T(x,y,t)\delta(xsin\phi + ycos\phi - k_\phi)dxdydt. \tag{3}$$

The two-dimensional function $P(k_\phi,t)$ as a function of k_ϕ and t (for a given value of ϕ) is the surface integral of T(x,y,t) over the plane for angle ϕ. The function $P(k_\phi,t)$ is also called a three-dimensional Radon transform of T(x,y,t).

Instead of using surface integration shown in Eq. 3, the maximum value projection method is to be applied in this implementation as follows.

$$P_m(k_\phi,t) = \mathbf{Max}_{t=0}^{L-1}[T(x,y,t)\delta(xsin\phi + ycos\phi - k_\phi)] \tag{4}$$

For a three-dimensional target trajectory T(x,y,t), $P_m(k_\phi,t)$ denotes a set of parallel projections taken along a series of parallel planes defined by the Dirac delta function. The function $P_m(k_\phi,t)$, as a function of k_ϕ and t for a given value of ϕ, is referred as the parallel projection of the three-dimensional target trajectory T(x,y,t) for angle ϕ.

The number of projections is arbitrary. Theoretically, increasing the number of projections improves the performance of the estimation, but increases the cost of computation. Assuming the number of projections is N, the angle increment

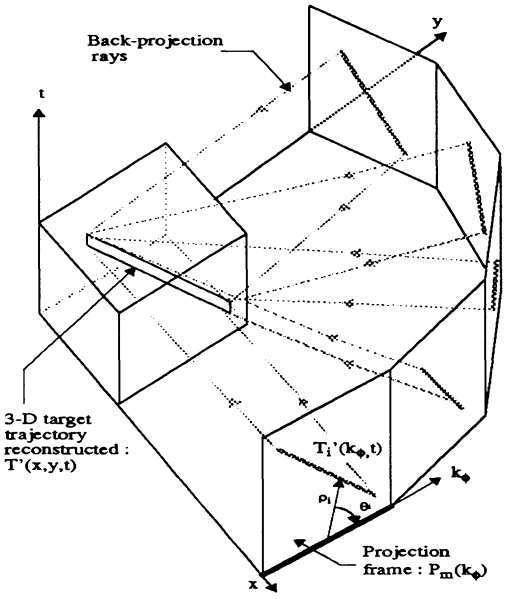

Figure 3: Reconstruction using Radon-like parallel line back-projection.

between projections is

$$\Delta\phi = \frac{90°}{N-1}. \tag{5}$$

Thus, the projection angle is

$$\phi = i \cdot \Delta\phi \text{ for } i = 0, 1, ...N-1. \tag{6}$$

In this work, the projection angle is assumed to be within the range from 0° to 90° with respect to the x-axis.

Once a series of the parallel projections is obtained using the forward projection defined by Eq. 4, the target track line parameters for each of the parallel projection frames are estimated by using the 2-D Hough transform equations. An estimate of the target trajectory in 3-D is obtained by back-projecting the N sets of 2-D track parameter estimates $(\rho_i, \theta_i)_{i=0,1,...N-1}$.

The back-projection shown in Figure 3 is defined as follows

$$T'(x,y,t) = \bigcap_{i=0}^{N-1} [T_i'(k_\phi,t)\delta(x sin\phi + y cos\phi - k_\phi),\ \forall t]. \tag{7}$$

where $T_i'(k_\phi,t)$ is the estimated two-dimensional target track function obtained by using the inverse Hough transform and $T'(x,y,t)$ is the reconstructed three-dimensional target trajectory function using parallel back-projection along a series of parallel back-projection planes defined by the Dirac delta function.

The accuracy of the three-dimensional target track estimation solution is limited by the input image frame signal-to-noise ratio and the discretization errors (data sampling and quantization). Discretization errors occur when the data is recorded discretely and when there is a projection onto a plane that is not parallel to one of the spatial or temporal planes.

2.1 Analytic Bounds on the Hough Space Errors

In the following, a derivation of the analytical bounds on the Hough space parameter errors that are introduced by image space noise contamination is presented. This provides a mechanism for quantitatively assessing track estimation performance of the projection-based algorithm. Assume a 3-D volume of image data is generated from a time-sequence of 2-D image frames. A set of 2-D projection data is then generated from the 3-D volume. The following analysis is applicable to the data contained in any 2-D of the projected frames. In this analysis the dominant noise sources are assumed to be thermal noise and discretization (sampling and quantization) noise.

A target track (line) in a 2-D projected frame is modeled by:

$$\rho_i = x_i \cos\theta_i + y_i \sin\theta_i \tag{8}$$

where x_i and y_i are the image domain coordinates for an arbitrary 2-D projection and ρ_i and θ_i are the corresponding Hough domain parameters. If the data are noisy, there will be errors in the estimates of the Hough domain parameters. The objective of this section is to determine the bounds on the errors for ρ_i and θ_i.

An error in the estimate of the Hough parameters ρ_i and θ_i will result in an error in the estimated target track. An estimated target track will fall within some neighborhood (noise strip) of the actual target track location. Here, it is assumed that the sampling grid is rectangular in the image plane with the pixel dimensions given by Δx_i and Δy_i.

The estimate of an actual target point x_i and y_i is given by:

$$\overline{x_i} = x_i + \epsilon_1 \tag{9}$$

$$\overline{y_i} = y_i + \epsilon_2 \tag{10}$$

where ϵ_1 and ϵ_2 are assumed to be zero mean, additive white Gaussian noise. Suppose

$$|\epsilon_1| \leq K\Delta x_i \tag{11}$$

$$|\epsilon_2| \leq K\Delta y_i \tag{12}$$

where K is a constant. The worst case estimates occur when $\theta_i = 45°$, $135°$, or $315°$. (For this application, tracks along $225°$ are not included because those correspond to movement along a path backward in time.) For these cases, the estimated track points could lie as far as $K\sqrt{\Delta x_i^2 + \Delta y_i^2}$ away from the actual track point. In general, the amount of error will depend on the geometry of the track.

2.2 Error Bound on $\overline{\rho_i}$

A bound on the estimate of ρ_i can be specified as a function of θ_i as follows:

$$(x_i \mp K\Delta x_i)\cos\theta_i + (y_i - K\Delta y_i)\sin\theta_i \leq \overline{\rho_i} \leq (x_i \pm K\Delta x_i)\cos\theta_i + (y_i + K\Delta y_i)\sin\theta_i \tag{13}$$

where $\overline{\rho_i}$ is the estimate of ρ_i. Consider the problem geometry shown in Figure 4. Here

$$\rho_{iU} \equiv \text{upper bound of estimate } \overline{\rho_i}$$

$$\rho_{iL} \equiv \text{lower bound of estimate } \overline{\rho_i}$$

The bound on the estimate of ρ_i is derived as follows:

(1) For $0 \leq \theta \leq \frac{\pi}{2}$:

$$\rho_{iU} = (x_i + K\Delta x_i)\cos\theta_i + (y_i + K\Delta y_i)\sin\theta_i \tag{14}$$

$$\rho_{iL} = (x_i - K\Delta x_i)\cos\theta_i + (y_i - K\Delta y_i)\sin\theta_i \tag{15}$$

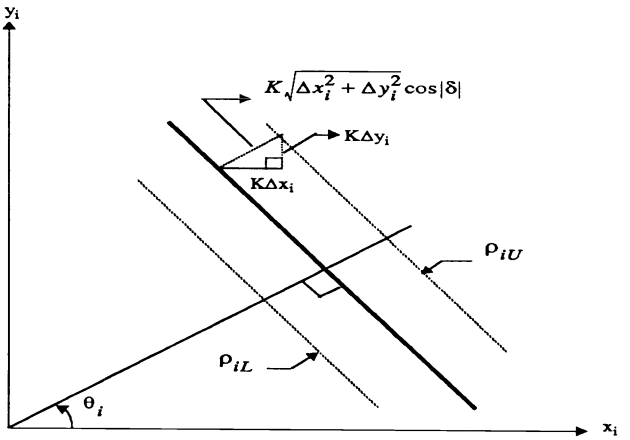

Figure 4: Geometry associated with determining error bounds on ρ_i of target track.

and

$$\rho_{iL} \leq \overline{\rho_i} \leq \rho_{iU} \tag{16}$$

where

$$\overline{\rho_i} = (x_i + \epsilon_1)\cos\theta_i + (y_i + \epsilon_2)\sin\theta_i \tag{17}$$

Then,

$$|\Delta\rho_i| = |\rho_i - \overline{\rho_i}| = \sqrt{\epsilon_1^2 + \epsilon_2^2}\cos|\theta_i - 45°| \tag{18}$$

and

$$|\Delta\rho_i| \leq |\rho_i - \overline{\rho_{iU}}| = |\rho_i - \overline{\rho_{iL}}| = K\sqrt{\Delta x_i^2 + \Delta y_i^2}\cos|\theta_i - 45°| \tag{19}$$

(2) For $\frac{\pi}{2} < \theta_i < \pi$:

$$\rho_{iU} = (x_i - K\Delta x_i)\cos\theta_i + (y_i + K\Delta y)\sin\theta_i \tag{20}$$

$$\rho_{iL} = (x_i + K\Delta x_i)\cos\theta_i + (y_i - K\Delta y_i)\sin\theta_i \tag{21}$$

and

$$|\Delta\rho_i| \leq K\sqrt{\Delta x_i^2 + \Delta y_i^2}\cos|\theta_i - 135°| \tag{22}$$

(3) For $\frac{3\pi}{2} < \theta_i < 2\pi$:

$$\rho_{iU} = (x_i + K\Delta x_i)\cos\theta_i + (y_i - K\Delta y_i)\sin\theta_i \tag{23}$$

$$\rho_{iL} = (x_i - K\Delta x_i)\cos\theta_i + (y_i + K\Delta y_i)\sin\theta_i \tag{24}$$

and

$$|\Delta\rho_i| \leq K\sqrt{\Delta x_i^2 + \Delta y_i^2}\cos|\theta_i - 315°| \tag{25}$$

Combining these three results, we can write:

$$|\Delta\rho_i| \leq K\sqrt{\epsilon_1^2 + \epsilon_2^2}\cos|\delta| \tag{26}$$

where,

$$\delta = \begin{cases} \theta_i - 45°, & for 0 \leq \theta_i \leq \frac{\pi}{2} \\ \theta_i - 135°, & for \frac{\pi}{2} < \theta_i < \pi \\ \theta_i - 315°, & for \frac{3\pi}{2} < \theta_i < 2\pi \end{cases} \tag{27}$$

If we assume $\epsilon = \epsilon_1 = \epsilon_2 \leq K\Delta x_i = K\Delta y_i = K$, (that is, $\Delta x_i = \Delta y_i = 1$) then,

$$|\Delta\rho_i| \leq K\sqrt{2}\cos|\delta| \tag{28}$$

If the track line is detectable in the noise strip and $K = 0.5$ and $0 \leq \theta \leq \frac{\pi}{2}$, the worst case error in ρ_i is:

$$|\Delta\rho_i| \leq \sqrt{2}cos\,|45° - 45°| = \sqrt{2} \tag{29}$$

Thus, $\overline{\rho_i}$ lies within a ± 2 pixel strip. For $K = 1.0$,

$$|\Delta\rho_i| \leq 2\sqrt{2} \tag{30}$$

and $\overline{\rho_i}$ lies within a ± 3 pixel strip.

2.3 Error Bound on $\overline{\theta_i}$

Assuming the length of the actual target track is L, determine the upper and lower estimation error bounds on $\overline{\theta_i}$, with δ defined as in Eq. 27. The error bound for $\overline{\theta_i}$ can be expressed as follows:

$$|\Delta\theta_i| = |\theta_i - \overline{\theta_i}| = \left|\frac{\pi}{2} - \tan^{-1}\left(\frac{2L}{\sqrt{\epsilon_1^2 + \epsilon_2^2}\cos|\delta|}\right)\right| \tag{31}$$

Again consider the case when $\epsilon = \epsilon_1 = \epsilon_2 \leq K\Delta x_i = K\Delta y_i = K$. Then,

$$|\Delta\theta_i| = \left|\frac{\pi}{2} - \tan^{-1}\left(\frac{2L}{\sqrt{\epsilon_1^2 + \epsilon_2^2}\cos|\delta|}\right)\right| \tag{32}$$

or

$$|\Delta\theta_i| \leq \left|\frac{\pi}{2} - \tan^{-1}\left(\frac{2L}{K\sqrt{2}\cos|\delta|}\right)\right| \tag{33}$$

A table of the *worst case errors* for $\overline{\theta_i}$ is shown below for $K = 0.5$ and $K = 1$. The results hold for $\theta_i = 45°, 135°$ or $315°$.

	L					
K	5	10	15	20	30	40
0.5	$\sim 15°$	$\sim 8°$	$\sim 5°$	$\sim 4°$	$\sim 3°$	$\sim 2°$
1.0	$\sim 29°$	$\sim 16°$	$\sim 11°$	$\sim 8°$	$\sim 5°$	$\sim 4°$

2.4 Simulation Results

The 3-D data set that is composed of real infrared unclassified data provided by NRL (HiCamp) with a number of simulated trajectories and various amounts of additive noise. The data set has a frame size of 32x32 pixels and up to 45 frames in the temporal direction in order to accommodate the longest possible track of a target moving at a speed of one pixel per frame. Simulations have been run to evaluate the performance of the algorithm at a number of signal-to-noise ratios and projections. The results indicate good performance down to 0dB with 5-9 projections and 15-20 frames of data. At low SNRs, performance degrades as the number of frames decrease and/or the number of projections decrease.

3. OPTIMAL 3-D DETECTION THEORY APPROACH

The 3-D detection theory algorithm is based on a binary hypothesis problem model. Once it has been decided that a target is present in the field of view, a procedure for estimating the location of the trajectory based on a calculation of the *a posteriori* probabilities of all possible trajectories is feasible. Here the solution is formulated so that multiple parallel target trajectories can be detected. Although, the extension to 3-D has been previously dismissed as too computation and memory intensive, recent advances in hardware capabilities now make it viable. The key to using the 3-D algorithm in a computationally efficient manner is to calculate the *a posteriori* probabilities recursively from the old *a posteriori* probabilities and the new frame of data. When a new frame is received, incomplete trajectories are updated and complete trajectories are replaced by new trajectories following the same paths.

At any instant of time, m, the stack of observation data, $X_{m-L+1,\ldots,m}$, consists of L frames. The detection problem can be set up as a binary hypothesis problem:

$$\begin{aligned} H_0 &: X_{m-L+1,\ldots,m} = N_{m-L+1,\ldots,m} \\ H_1 &: X_{m-L+1,\ldots,m} = \sum_{(\rho_i,n_j)\in\mathcal{R}} S_{m-L+1,\ldots,m}(\rho_i, n_j, \theta) + N_{m-L+1,\ldots,m} \end{aligned}$$

A track in a stack of frames is characterized by (1) its spatial parameters, ρ_i and θ, and (2) the time it entered the field of view, indicated by frame number n. ρ_i takes on the value 1 when a track is present at the ith value and 0 otherwise, and thus serves as an indicator for track locations in ρ space. $\mathcal{R}$ is the set of parameters, (ρ_i, θ, n_j), that indicates the set of trajectories present. Here $\sum_{(\rho_i,n_j)\in\mathcal{R}} S_{m-L+1,\ldots,m}(\rho_i, n_j, \theta)$ is the signal in the stack of L frames. The pixels corresponding to the trajectories in set $\mathcal{R}$ are equal to one with all other pixel values equal to zero. $N_{m-L+1,\ldots,m}$ is a stack of frames representing the pixels of noise in the most recent L frames. The problem of detection is to decide whether there is noise alone in the data, in which case hypothesis H_0 is true, or there are one or more tracks and noise in the data, in which case H_1 will be true.

It is well known that thresholding the likelihood ratio of the received data provides optimal detection performance. The likelihood ratio is the ratio of the probability density functions of the data under the hypothesis H_1 and H_0, that is,

$$\Lambda(X_{m+L+1,\ldots,m}) = \frac{p(X_{m+L+1,\ldots,m}|H_1)}{p(X_{m+L+1,\ldots,m}|H_0)}$$

Using the law of total probability for a discrete case this can be expanded for all possible patterns of parallel target trajectories as,

$$\Lambda(X_{m+L+1,\ldots,m}) = \sum_{\theta,\rho_i,n_j} \Lambda(X_{m+L+1,\ldots,m}|\rho_i, n_j, \theta) P(\rho_i, n_j, \theta|H_1) \tag{34}$$

The problem with parallel multiple trajectories whose number is not known is that the number of patterns of possible parallel trajectories is immense. For example, in a data consisting of a stack of 20 frames each with 33×33 pixels the number of possible patterns of parallel trajectories in each direction is approximately equal to $2^{33\times(33+20)}$. This is the number of terms in the summation in equation (34). This complexity can be greatly reduced if we assume that the parallel target trajectories are independent of each other, a reasonable assumption to make if we exclude the possibility of trajectories overlapping each other.

Let $P(\rho_i = 1|\theta, H_1) = p_\rho$ be the *a priori* probability of a trajectory being present at $\rho = \rho_i$ for a given θ. Similarly, let $P(n_j = 1|\theta, H_1) = p_n$ be the *a priori* probability that a trajectory enters the field of view at frame n_j. Based on the independence of ρ_i and the frame number n, we can write the following joint probabilities

$$\begin{aligned} P((\rho_i, n_j) = 1|\theta, H_1) &= P(\rho_i = 1, n_j = 1|\theta, H_1) = p_\rho \times p_n \\ P((\rho_i, n_j) = 0|\theta, H_1) &= P(\rho_i = 1, n_j = 0|\theta, H_1) + P(\rho_i = 0, n_j = 1|\theta, H_1) \\ &\quad + P(\rho_i = 0, n_j = 0|\theta, H_1) \\ &= 1 - p_\rho \times p_n \end{aligned}$$

The above arguments can be used to greatly reduce the complexity of equation (34). After some algebraic manipulation, this equation can be written as a sum of products of $(N \times R)$ factors

$$\Lambda(X) = \sum_{\theta} P(\theta|H_1) \prod_{i=1}^{N} \prod_{j=1}^{R} [\Lambda(X|n_i, \rho_j, \theta) P((n_i, \rho_j) = 1|\theta, H_1) + P((n_i, \rho_j) = 0|\theta, H_1)] \tag{35}$$

Since the parameters ρ and n are independent of each other, the above expression can be written as

$$\begin{aligned}
\Lambda(X) &= \sum_{\theta} P(\theta|H_1) \prod_{i=1}^{N} \left[\prod_{j=1}^{R} [\Lambda(X|n_i, \rho_j, \theta) P(\rho_j = 1|\theta, H_1) + P(\rho_j = 0|\theta, H_1)] \right] P(n_i = 1|\theta, H_1) \\
&\quad + P(n_i = 0|\theta, H_1) \\
&= \sum_{\theta} P(\theta|H_1) \prod_{j=1}^{R} \left[\prod_{i=1}^{N} [\Lambda(X|n_i, \rho_j, \theta) P(n_i, = 1|\theta, H_1) + P(n_i, = 0|\theta, H_1)] \right] P(\rho_j = 1|\theta, H_1) \\
&\quad + P(\rho_j = 0|\theta, H_1)
\end{aligned}$$

The conditional likelihood ratios $\Lambda(X|n_i, \theta)$, $\Lambda(X|\rho_j, \theta)$ and $\Lambda(X|\theta)$ are then defined as,

$$\Lambda(X|n_i, \theta) = \prod_{j=1}^{R} [\Lambda(X|n_i, \rho_j, \theta) P(\rho_j = 1|\theta, H_1) + P(\rho_j = 0|\theta, H_1)] \tag{36}$$

$$\Lambda(X|\rho_j, \theta) = \prod_{i=1}^{N} [\Lambda(X|n_i, \rho_j, \theta) P(n_i, = 1|\theta, H_1) + P(n_i, = 0|\theta, H_1)] \tag{37}$$

and

$$\Lambda(X|\theta) = \prod_{i=1}^{N} \prod_{j=1}^{R} [\Lambda(X|n_i, \rho_j, \theta) P((n_i, \rho_j) = 1|\theta, H_1) + P((n_i, \rho_j) = 0|\theta, H_1)] \tag{38}$$

$$= \prod_{i=1}^{N} [\Lambda(X|n_i, \theta) P(n_i = 1|\theta, H_1) + P(n_i = 0|\theta, H_1) \tag{39}$$

$$= \prod_{j=1}^{R} [\Lambda(X|\rho_j, \theta) P(\rho_j = 1|\theta, H_1) + P(\rho_j = 0|\theta, H_1) \tag{40}$$

It is seen from the above formulation that the conditional likelihood ratio $\Lambda(X|n_i, \rho_j, \theta)$ is the basic building block for computing all other likelihood ratios, conditional or otherwise. In fact, the 3-D Hough transforms are embedded in this term. Also, this algorithm can be computed recursively following the procedure given by Hunt et al. [3].

3.1 3-D Track Location Estimation

Once the tracks are detected, the problem of estimating the parameters that characterize these tracks remains to be solved. Given a data set, using the Bayesian framework for estimation, determine the *a posteriori* probabilities of the parameters (ρ_i, θ, n_j). The estimation problem is developed in two stages. In the first stage, the *a posteriori* probabilities conditional to the angle of orientation, θ, are computed. In the second stage, the *a posteriori* probability of the angle, θ, is computed.

Assume that the presence or absence of a track at each possible position ρ_i, for a target that entered the field of view at frame n_i conditional to a given θ, is statistically independent *a priori*. The *a priori* probability for any pattern

of parallel tracks is shown below (where b is either 1 or 0 indicating the presence or the absence of a track at that location).

$$p\left[(\rho_1, n_1,) = b, \ldots, (\rho_1, n_{N(\theta)}) = b, (\rho_{P(\theta)}, n_1) = b, \ldots, (\rho_{P(\theta)}, n_{N(\theta)}) = b|\theta, H_1\right]$$
$$= \prod_{j=1}^{N(\theta)} \prod_{i=1}^{P(\theta)} p\left[(\rho_i, n_j) = b|\theta, H_1\right]$$

Then $p(\rho_i, n_j = 1|\theta, H_1)$ represents the *a priori* probability of a target present that entered the field of view at frame n_j at position ρ_i, conditional to a given angle θ and the H_1 hypothesis. Assume that the parallel tracks are independent of each other in the sense that the presence or absence of a track at a location has no influence on the presence or absence of a track at other parallel locations, the above result holds good even *a posteriori*. Thus,

$$p\left[(\rho_1, n_1,) = b, \ldots, (\rho_1, n_{N(\theta)}) = b, (\rho_{P(\theta)}, n_1) = b, \ldots, (\rho_{P(\theta)}, n_{N(\theta)}) = b|\theta, X, H_1\right]$$
$$= \prod_{j=1}^{N(\theta)} \prod_{i=1}^{P(\theta)} p\left[(\rho_i, n_j) = b|\theta, X, H_1\right]$$

Following the Bayesian framework one can write the *a posteriori* probabilities for ρ and n conditional to θ as

$$P(\rho_j = 1|\theta, X, H_1) = \frac{\Lambda(X|\rho_j, \theta)P(\rho_j = 1|\theta, H_1)}{\Lambda(X|\rho_j, \theta)P(\rho_j = 1|\theta, H_1) + P(\rho_j = 0|\theta, H_1)} \tag{41}$$

and

$$P(n_i = 1|\theta, X, H_1) = \frac{\Lambda(X|n_i, \theta)P(n_i = 1|\theta, H_1)}{\Lambda(X|n_i, \theta)P(n_i = 1|\theta, H_1) + P(n_i = 0|\theta, H_1)} \tag{42}$$

The *a posteriori* probability of the angle of orientation can be written as

$$p(\theta|X, H_1) = \frac{\Lambda(X|\theta)p(\theta|H_1)}{\Lambda(X)} \tag{43}$$

The forms of the *a posteriori* probabilities indicate that they can be easily computed once the conditional likelihood ratio term is computed.

3.2 Estimation of Parameters ρ_i, θ and n

Presented below are simulation results for the parameter estimation case. Equations (41), (42) and (43) provide a frame work for estimating the three parameters that characterize a moving target. Figure 5 shows the results at the end of frame 35, for the case when three targets enter the field of view at frames $n = 5, 10$ and 15 with ρ_0 at an angle of $\theta = 45^0$. The figure shows three sets of results at a pixel SNR of -6.8db, -3.8db and 0.8db. The figures on the left are the plots of $P(\rho_j = 1|\theta, X, H_1)$, the figures in the middle are $P(n_i = 1|\theta, X, H_1)$ and on the right are the plots of $P(\theta|X, H_1)$.

With increasing SNR the plots become less noisy and the peaks get more and more well defined. For example, at SNR = 0db, in both the $P(\rho_j = 1|\theta, X, H_1)$ and $P(n_i|\theta, X, H_1)$ plots, along $\theta = 45^0$, there are peaks at locations $\rho_i = 0$ and $n = 5, 10$ and 15. This indicates a high probability of tracks being present at these parameter values.

With the help of these plots one could compute the *a posteriori* probability of a particular pattern of tracks. For example, we can multiply the peaks exceeding the value 0.5 on the $P(n_i = 1|\theta, X, H_1)$ plot along $\theta = 45^0$, and multiply the product with $P(\theta|X, H_1)$ for $\theta = 45^0$ to compute the marginal *a posteriori* probability for a pattern formed by the tracks that entered at these n's and $\theta = 45^0$ for all values of ρ_i. Similarly, we can compute the marginal probability of ρ_i and θ with the information available in the $P(\rho_i = 1|\theta, X, H_1)$ and $P(\theta|X, H_1)$ plots.

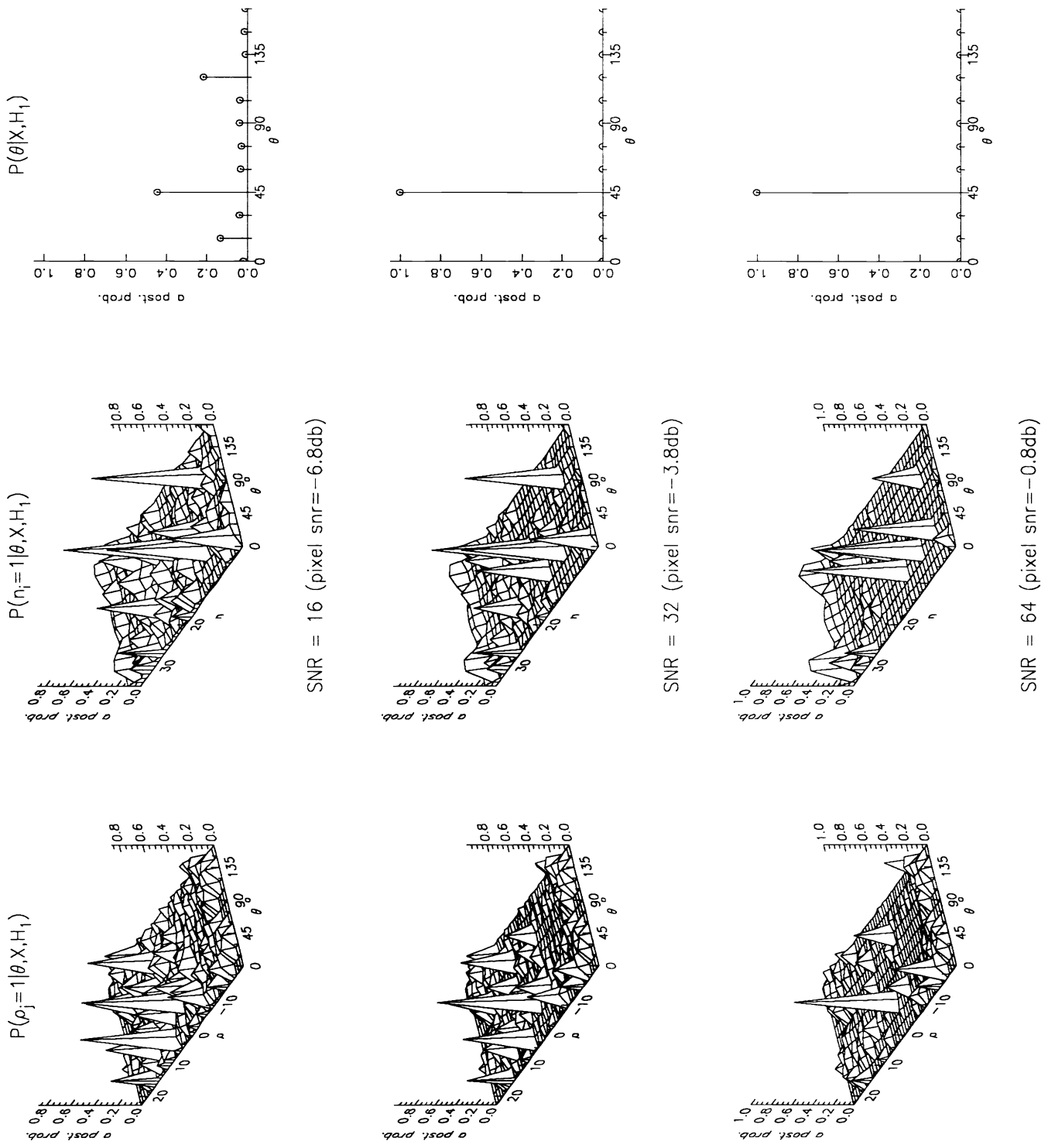

Figure 5: 3-D *A Posteriori* Probability Algorithm - Frame 35

4. CONCLUSIONS

In this paper two methods for tracking dim, unresolved target tracks were presented. In the first case, a projection-based Hough transform algorithm was developed. This algorithm processes a set of 2-D projected frames of data to obtain the estimates of the track parameters. In the second case, a signal detection/estimation theory technique was developed. The detection algorithm decides between noise alone and the presence of multiple parallel trajectories in noise. The estimation algorithm determines the location of the detected parallel tracks. A mix of uncertainties in orientation, location and the number of parallel tracks in the image was considered. The relationship between both the structure and performance of optimal *a posteriori* probability algorithms and the Hough transform was obtained.

5. ACKNOWLEDGEMENTS

This research was funded by the Naval Research Laboratory under contract N0014-90-K-2019 to the Research Triangle Institute. Special thanks are extended to W. Howard Ruedger (formerly with Research Triangle Institute) and to the graduate students who worked on the project: Jae-Ho Choi (North Carolina State University), John Gostomski (formerly at Duke University), and Mark Rahmes (Duke University) for their contributions to this work.

References

[1] A.E. Cowart, Wesley E. Snyder, and W. Howard Ruedger. The detection of unresolved targets using the Hough transform. *Computer Vision, Graphics, and Image Processing*, 21:222–238, 1983.

[2] Mary L. Padgett, Sarah A. Rajala, Wesley E. Synder, and W. Howard Ruedger. Detection of manuevering target tracks. *Proceedings of SPIE*, 575:145–155, August 1985.

[3] Douglas J. Hunt, Loren W. Nolte, and W. Howard Ruedger. Performance of the hough transform and its relationship to statistical detection theory. *Computer Vision, Graphics, and Image Processing*, 43(2):221–238, August 1988.

[4] Douglas J. Hunt, Loren W. Nolte, Amy R. Reibman, and W. Howard Ruedger. Hough transform and signal detection theory performance for images with additive noise. *Computer Vision, Graphics, and Image Processing*, 52(6):386–401, December 1990.

[5] Loren W. Nolte, Sarah A. Rajala, W. Howard Ruedger, and Douglas J. Hunt. Signal detection theory and the hough transform. In *Proceedings of the Naval Research Laboratory Seminar on Algorithms for Autonomous Passive Surveillance*, February 1989.